ISME

Experimental Investigation of Wake on an Elliptic Cylinder in the Presence of Tripping Wire

A.A. Bakkhoshnevis[*]
Associate Professor

A.R. Mamouri[†]
Ph.D. Student

S. Nazari[‡]
M.Sc. Student

In this research, the behavior and characteristics of the wake of flow in an elliptic cylinder with zero angle of attack in the presence of a tripping wire were investigated experimentally. For this purpose, the used an Aluminum cylinder with an elliptical cross section of the major and minor axis of 42.4 mm and 21.2 mm, respectively, and of the height of 390 mm. The cylinder model was examined in the test section of a blower type wind tunnel. The Reynolds numbers of the experiment for the major axis are 25700 and 51400 for 10 m/s and 20 m/s speeds, respectively. Tripping wires of the diameter of 0.5 mm, 1 mm, and 1.5 mm placed symmetrically at both sides of the cylinder, each are tested at angles of zero, 23.7, and 40.9 degrees with respect to the stagnation point. The drag coefficient for the smooth cylinder for either of the Reynolds numbers is about 0.6. The results indicate that in the best possible case, the drag coefficient for the 0.5 mm wire reduces by 75%. In the best cases, it also reduces by 56.9% and 65.5% for the 1 mm and the 1.5 mm wires, respectively.

Keywords: Trip wire; Drag coefficient; Wake of elliptic cylinder; Hot wire anemometry.

1 Introduction

Aerodynamics of the flow around circular and elliptical cylinders and their industrial applications is an important and prevalent case of study. On the other hand, decrement of the drag coefficient has many applications in science and industry. Decrement of the drag coefficient in industries leads to less fuel consumption, better heat transfer, less noise, more speed, more stable structures, etc. This is while the boundary layer and its separation has a big role in aerodynamics of cylinders and its separation is always tried to be avoided or delayed in order for a higher efficiency. This can optimize the drag coefficient.

[*]Corresponding Author, Associate Professor, Deptartmant of Mechanical Engineering, Hakim Sabzevari University, Sabzevar, Iran khosh1966@yahoo.com

[*] Ph.D. Student, Hakim Sabzevari University, Sabzevar, Iran amirelmir3000@yahoo.com

[‡] M.Sc. Student, Hakim Sabzevari University, Sabzevar, Iran pixy64@gmail.com

There are various methods for avoiding or delaying the separation of the boundary layer. The methods include blade-like vortex generators, surface roughness, tripping wire, air flow ionization, injecting or suctioning the fluid over the surface, etc. Applications of elliptical cylinders include the pipes used in thermal converters, attack layer of a flap in a multi-part airfoil, etc. Igarashi[1] did a series of experimental studies on the flow around a circular cylinder in a range of sub-critical Reynold numbers under the influence of vortex generator. In this research, the drag coefficient reduces by %53.8 in the best case. Igarashi[2] did an experimental study of a circular cylinder in which the effect of the tripping wire is present in transmission of the boundary layer. In this study, the drag coefficient reduced by %70 in the best case. Aiba et al[3] showed the effect of tripping wire in heat transfer around a circular cylinder. A pair of wires were placed symmetrically on the cylinder at 65 degrees. They showed that decreasing the drag coefficient increases the Naslet number and consequently the heat transfer increases. Zhou et al[4] studied the effects of three types of tripping wires near the stagnation point on a circular cylinder. Every pair of wires were placed symmetrically at a distance from the cylinder. Their results showed that the drag coefficients increase for $\mathrm{Re} = 200$ at $\alpha = 40^{\circ}$ by %18 and for $\mathrm{Re} = 5.5 \times 10^4$ at $\alpha = 30^{\circ}$ by %59.

Missirlis et al[5] in an experimental ad numerical research, demonstrated the application of elliptical cylinder in a heat exchanger. The results of using an elliptical cylinder showed an improvement in pressure drop and heat transfer of the flow compared with circular cylinders. Hover et al [6] in a research on the effect of tripping wire on vortex-induced loads and vibration with just one pair of wires at the angle of 70 degrees showed that the drag coefficient reduces by about %50 compared with the cases without the wire. Fukudome et al[7] in an experimental and numerical research, studied the effect of a tripping wire at the stagnation point in an airfoil of a turbine blade. The results show that separation of the flow at higher angles of attack is delayed. Furthermore, the lift increases and the flow optimization improves.

Quadrante and Nishi[8] in an experimental research demonstrated the effects of tripping wire on oscillations of a circular cylinder. They derived the angles of the wires for the best and worst effects. Results show that at the angle of complete oscillations vanishing, the drag coefficient is minimum, while the value of Strouhal number does not have any significant variation in comparison with the plain cylinder. Raman et al[9] in a numerical study of elliptical cylinders showed that at a specific Reynold's number, with decreasing the axis ratio the drag coefficient decreases and Strouhal's number increases. Ota et al[10] studied the flow around an elliptical cylinder with the axis ratio of 1/3 experimentally.

In this research, the appropriate angle of attack for the happening of critical Reynold's number and consequently, the occurrence of the first turbulences behind the model was derived. Paul et al[11] conducted a numerical study of an elliptical cylinder, in which they studied the effects of the angle of attack, the axis ratio, and Reynold's number of a laminar and transient flow on the properties of the flux. Furthermore, the dependence of the flow parameters and the vortex shedding on the angle of attack is demonstrated in this research. Perumal et al[12] studied the effects of the blockage ratio, Reynold's number, and the length of the canal on the properties of the flux in an elliptical cylinder with the Lattice Boltzmann Simulation method. In this research, it was shown that the frequency of vortex shedding increases with increasing the blockage ratio.

In this research, the wake in an elliptical cylinder in the presence of tripping wires is studied experimentally. Considering the previously done researches on elliptical cylinders, the mean velocity, oscillatory velocities, and drag coefficient in elliptical cylinders in the presence of tripping wires has not been conducted yet.

2 Studied parameters

The turbulence intensity is an important parameter that determines the quality of the fluid flow. The turbulence intensity is expressed as:

$$\%Tu = \frac{\sqrt{\overline{\acute{u}^2}}}{U_{ref}} \times 100 \quad (1)$$

The dimensionless velocity defect is derived via

$$\frac{w_0}{U_{ref}} = \frac{U_{ref} - U_{min}}{U_{ref}} \quad (2)$$

Strouhal number is also a dimensionless number that denotes the intensity of the frequency of vortex shedding of the Carmen formed at behind the model and is defined as:

$$\mathrm{St} = {fd}/{U_{ref}} \quad (3)$$

If the elliptic cylinder is posed horizontally in the direction of the flow, the aspect ratio is defined as the minor diameter over the height of the gate of the wind tunnel. Based on the results of the researches on this subject, if for an elliptic cylinder the aspect ratio of less than 0.08 is chosen, the error of the experiments would be negligible. For more information refer to Alonso et al[13] or Flynn and Eisner[14].

$$\beta = {B}/{H} \leq 0.08 \quad (4)$$

In the conditions of this research, the aspect ratio β equal to 0.053.

3 Experimental setup

The hot wire anemometry is one essential instrument for measuring the instantaneous speed of the fluid flow. Considering the unique properties of this instrument, its main application is to do experiments for turbulence flow of gas or air. The anemometry used in this research is of the constant temperature type, which is able to measure the mean velocity, turbulences, and the frequency of the vortexes going out from behind the model. The wind tunnel of this experiment is of the open-circuit blowing type, which uses a 7kW engine which is able of producing an air flow of the velocity of 30 m/s. the test section of this tunnel is of plexiglas material of the length of 168 cm, width of 40 cm, and the height of 40 cm. The turbulences intensity in free flow in the test section in absence of any model is shown for both the velocities of the flow in the Figure (1).
The one dimensional probe used in this experiment has a sensor of the length of 1 mm and the diameter of 5μm. To move the probe at different points an accurate mechanism with three degrees of freedom is used. The accuracy of this mechanism is 0.01 mm. Schematic view of the wind tunnel is shown in the Figure (2).

Constant-temperature electronic circuit is a main part of the hot-wire anemometer device. This circuit is designed in such a way that it automatically equalizes the Watson Bridge. The anemometer used in this study is of the constant-temperature type. Schematic view of that is shown in the Figure (3).

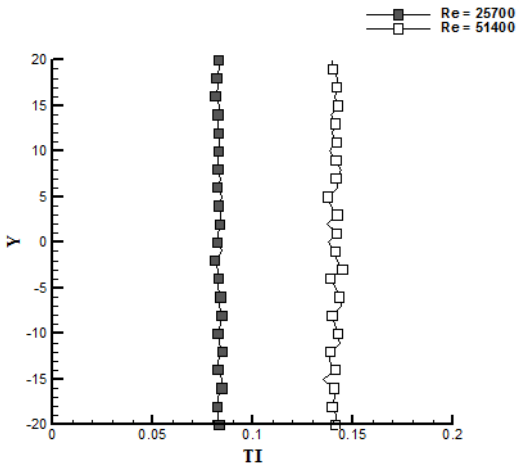

Figure 1 intensity of turbulences of free flow in the test section

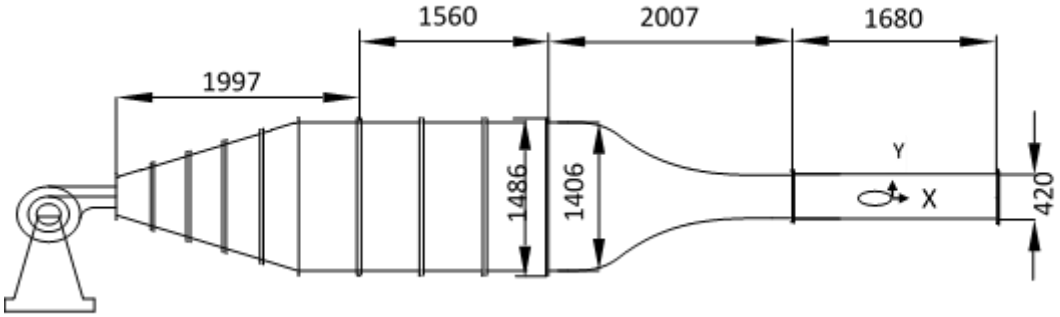

Figure 2 Schematic view of the wind tunnel.

In order to transmit the output signals of the CTA electronic circuit to the computer via the DAQ card without any problems and also to suppress electronic noises in the output signals and remove them as far as possible, we need a signal conditioner unit that is shown in the Figure (4). The probe sensor of the anemometer is of the hot-wire type and has a diameter of about 5 µm, which has a high frequency response. Schematic view of probe is shown in the Figure (5).

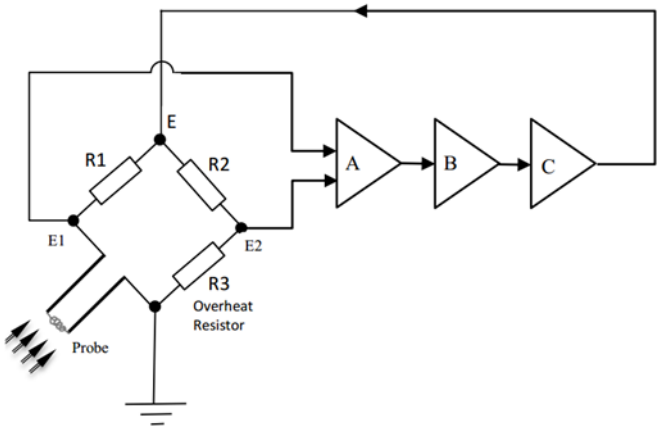

Figure 3 Schematic view of the Constant-temperature electronic circuit.

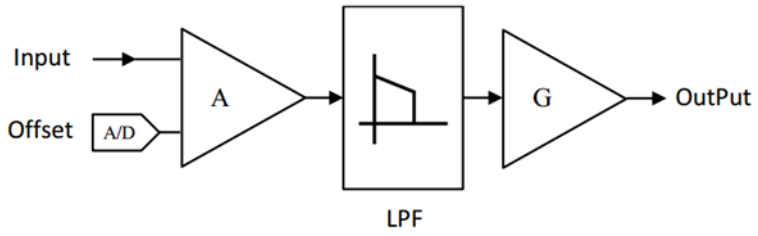

Figure 4 Schematic view of the Constant-temperature electronic circuit.

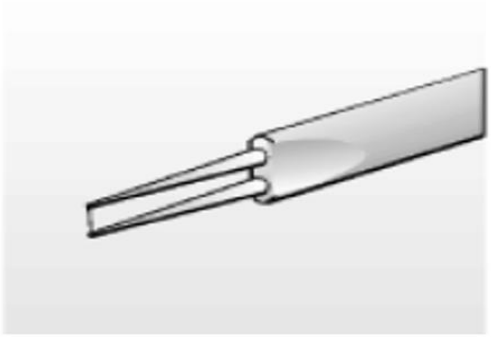

Figure 5 Schematic view of the probe.

The program that controls and mediates between all the units of the anemometer is Farasanj Saba's company Rake flow ware. As mentioned, in this research the wake of an elliptical cylinder at the zero horizontal angle of attack in the presence of the tripping wire is studied. An Aluminum cylinder of the height of 390 mm, major axis of 42.4 mm, and minor axis of 21.2 mm is used. The data collecting stations in the order of the ratio of distance from the model to the minor axis are: X/B = 1, 2.5, 5, 10, 15, 20, 25 that is shown in the Figure (6).
Tripping wires of diameters of 0.5 mm, 1 mm, and 1.5 mm are chosen, each of which are symmetrically tested at three different positions of zero, 23.7, and 40.9 degrees with respect to the stagnation point. This mentioned model is tested at two Reynold's numbers of 25700 and 51400 for the speeds of 10 m/s and 20m/s, respectively.

4 Results and discussion

As mentioned, in this research we studied the wake of an elliptical cylinder with zero angle of attack in the presence of tripping wires at seven different longitudinal positions and at Reynold's numbers of 25700 and 51400.

4.1 Distribution of the profile of the dimensionless velocity

The mean velocity profiles, though having the variant and transient nature of the turbulent velocity fluctuation components over a period, but are symmetric.

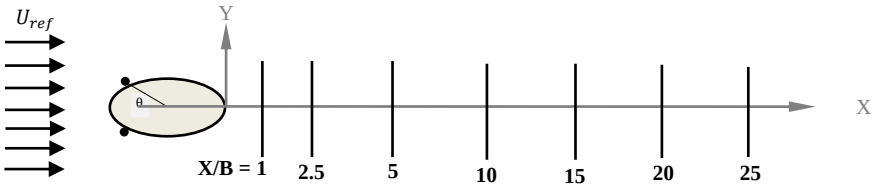

Figure 6 Schematic view of the model

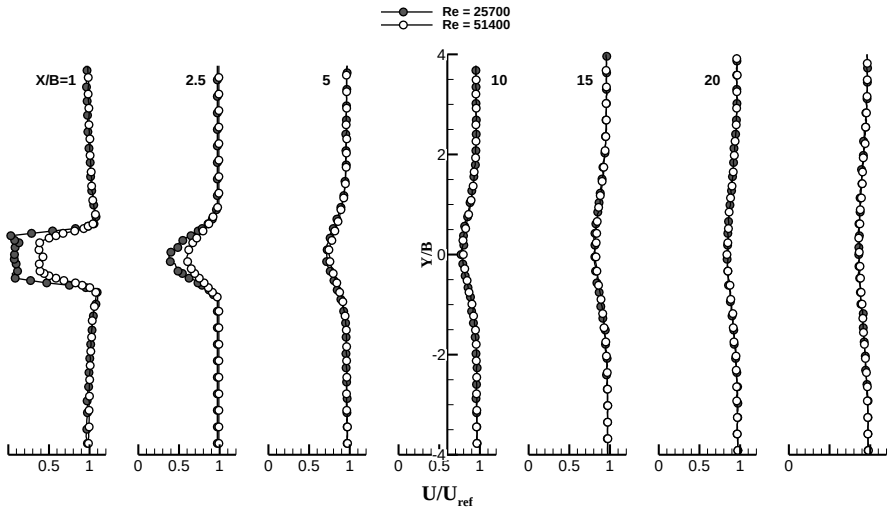

Figure 7 Distribution of the profile of the dimensionless mean velocity for smooth elliptic cylinder

As it's known, vortices form are instantaneously and asymmetrically behind the model, but as shown in Figure (7), even at the first stations of the near wake the sketched profiles of mean velocity are quite symmetric. Interpretation of this phenomenon is that the formation of vortices behind the cylinder is instantaneous and reoccurs periodically. Now, if the data timing at a position is longer than the period of the formation of the vortices, one can obtain the average speed at any point by calculating the time average of the speed at those points, which does not exhibit the asymmetric effects of instantaneous speed.

In Figure (7), the data timing is approximately 500 times the period of the formation of vortices. Another significant point that is seen in Figure (7) is the existence of two extremums in the speed profiles of near wake. The cause of this phenomenon can be traced to the momentum of the boundary layer formed at the surface of the model. In a way that in the layers near the model, the existing momentum of the boundary layer on the surface of the cylinder increases the energy and velocity of the nearby layers after the dissipation of the layer, where this phenomenon losses its affection at the farther layers behind the model and cannot affect the velocities of the fluid particles.

Another significant point is that increasing the distance from behind the cylinder, the difference between speeds inside and outside the wake decreases and the width of the wake increases, which eventually smoothens the profile of the mean velocity. At the near wake, because of the separation and returning flows, the flow drop is larger, which decreases by going away from the model and the flow inside the wake smoothens.

On the other hand, it is seen in Figure (7) that the profiles for the two Reynolds numbers become very close to each other from the $X/B = 5$ station onward. This is because the rate of dissipation of vortices at the Reynolds number of 25700 is more than that of 51400.
Furthermore, from this station onward, because of the changes in the behaviors of the flow, including the dissipation of returning flows, smoothening of the flow, and decrement of the effects of the separation of the flow from the first positions of data collecting to the last ones, the velocity inside the wake increases gradually, which changes the profiles of mean velocity toward becoming rather smooth ones at the last data collecting stations. For a smooth elliptic cylinder in absence of tripping wire, the fluid flowing over the surface makes a boundary layer, which later on separates from the surface. This separation causes the formation of a zone called the wake, which has different properties than the free flow, behind the cylinder.
On the other hand, when a flow jumper factor is placed at the path of the flow, significant changes occur for the properties of the boundary layer and the wake of the flow. In between, the tripping wire, as a flow jumper that is placed on the surface of the cylinder, causes a phenomenon called the transportation of the boundary layer. In fact, in presence of the tripping wire, because of the collision of the flow lines with the wire and so their upward deviation causes the flow to separate from the surface of the cylinder and land again at another point called the reattachment point down the flow. This point is where the boundary layer forms once again. All along forming the boundary layer, there is also a separation point. Then, because of the presence of the tripping wire, the boundary layer forms at a lower point downstream over the surface of the cylinder. Therefore, the wake that forms has a narrower width.
On the other hand, the tripping wire causes essential changes in the profile of mean velocity. Indeed, one should note that because of the large number of the curves, only the curves for the Reynolds number of 51400, which has more effects on the properties of the flow than the 25700 Reynolds number, are shown. The relatively positive effects of the wire on the properties of the flow in the wake behind the model increase the profile of mean velocity. This is more apparent at farther stations.
The condition of the wire, depending on its position, can have positive or negative effects on the properties of the flow. If placing the wire increases the width of the wake, strong vortices will form behind the model. In this case, the mean velocity in the wake decreases and the turbulences increase. Thus, the conditions for improving the flow diminish. However, if the width of the wake decreases in the presence of the tripping wire, the vortices behind the model become weaker and the conditions for improving the properties of the flow increase.[15]

In Figure (8), among the profiles of the dimensionless mean velocity at the $^{X}/_{B} = 1$ station it seen that the peak of the velocity at the layers near the model in the profiles of smooth cylinder is higher than those of other profiles. This is because the boundary layer on the smooth cylinder has a certain momentum, which increases the energy, and so the velocity, of the nearby layers. This phenomenon loses its effect at farther layers behind the model and this is why there is no peek at those latter stations. This is while for the wire at $\theta = 40.9^{\circ}$ this peek is much lower. The flow loses some momentum when colliding with the wire, which causes a dissipation of some momentum. Therefore it can be reasoned that formation of the reattachment point for the boundary layer cause a dissipation of some momentum of the flow of the boundary layer. Another point is that when the separation of the boundary layer happens at a farther point than upstream, a wake of a higher width forms. Thus stronger vortices form and the speed of the flow for them is less than other instants with less width.[15] This is more apparent in Figure (8) and station $^{X}/_{B} = 1$ for smooth profile. It is clear in this figure that for the profile related to $\theta = 40.9^{\circ}$ the velocity is more than other profiles, and so it has a better influence on the properties of the flow.

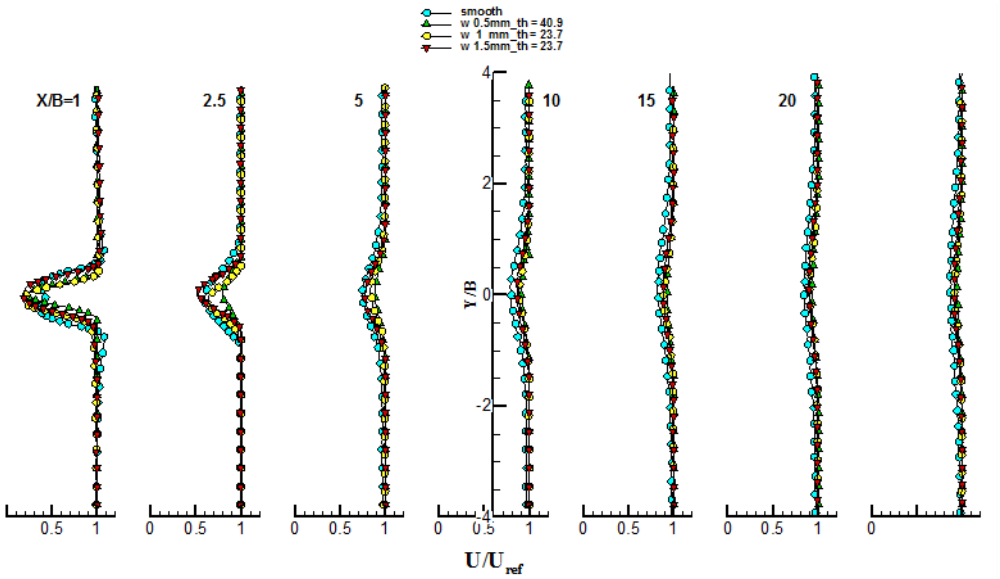

Figure 8 Distribution of the profile of the dimensionless mean velocity at different positions

Another point is that together with increasing the distance from the model, the width of the wake increases and the difference between the speeds in the wake and outside of it decreases. This is seen in Figure (8). In interpretation of why the wake vanishes with increasing the distance from behind the model, one can say that the shear layer of the wake is affected by the free flows and so the free flows try to vanish the shear layer under the name of the wake.

4.2 Profile of dimensionless velocity defect

The speed difference between the free-flow and the lowest speed in wake for each Station from the beginning they near the model to their end in a region away from the downstream has a reduction rate. The speed difference is called velocity defect.

As is clear from Figure (9), the velocity defect gradient profiles from the station $X/B = 5$ to the next for both profiles are identical and the two graphs are coincide. It shows that from this station to the next, mean velocity profiles are very close to each other, and this is defined in Figure (7). In two previous stations in Figure (9), it's known that the gradient for graph with Reynolds number 25700 is more than the gradient for others. A sharp gradient in velocity defect profile implies the rate of change of speed $\frac{\partial}{\partial x}(\Delta u)$. This parameter also correlates with the rate of dissipation. Therefore, the dissipation rate in this profile must be higher than the other that is detectable according to Figures (7), that the minimum amount of mean velocity profiles for Reynolds number 25700 on other stations away from the model matches with other speed profile for Reynolds number 51400. Because of the high mean velocity on the wake for wire with a diameter of 0.5 mm compared to the other profiles, it is necessary that in Figure (10) a sharp drop occur in velocity defect graph for wire with a diameter of 0.5 mm in order that the curve set under the other curves. The reason for this is that the rate of dissipation for the station near the model due to high gradient of velocity profiles in this case, is more than any other stations, thus moving away from the model, a sharp drop occurs in dimensionless velocity defect chart for this wire.

Another point is that the more closing of velocity defect curves to $1/x$ curves, conditions will be more optimal. Because for a curve in $1/x$ state, the speed difference on the wake is minimal. As a result, speed on the wake will be maximal.

4.3 Dimensionless turbulent intensity profile

The direct relation of energy dissipation with mean velocity gradient of $\partial\bar{u}/\partial y$ and also with gradient of turbulent velocity fluctuation component $\partial\acute{u}/\partial y$, respectively in Figures (7) and (11) suggests the fact that the wake of flow for Reynolds number 25700 has a faster growth of the dissipation. Hence, from the station $X/B = 5$ to the next, the mean velocity profiles and turbulence profiles related to the Reynolds number 25700, because of energy dissipation will close to profiles related to the Reynolds number 51400 and coincides on it.
On the other hand, as is clear, as we get away from the model the intensity gradient changes of dimensionless turbulences will decrease sharply. In Figure (11), two extremums are seen in profile of dimensionless turbulent intensity percent in Reynolds number 51400 in the station $X/B = 1$ that by moving away from the model, these two extremums disappear due to flow smoothly. It is due to eddy flows and swirling flows near the cylinder and steady flows far away from the cylinder.
According to Figures (7) and (11), a similar behavior is observed at each station. From that point of view that if in station $X/B = 5$ both mean velocity profiles are almost coincident, so the two turbulence profiles in the same station are nearly coincident. However, the mean velocity in Figure (7) on the wake is rising, but turbulences in Figure (11) on the wake are decreasing. This is due to the impact of energy dissipation on the characteristics of flow that takes place in such a way that increased mean velocity of $\bar{u}$ and reduced $\acute{u}$ turbulences of flow in wake is done with steady rates. In a way that rate of changes are the same.

The other thing that could be significant is that the peak of flow turbulences in turbulence profile in the wake behind the model, shows the conditions of a point of the wake that most turbulences of the flow going on in there. On the other hand, by drawing the mean velocity profile and multiplying the flow turbulences in a chart, turbulences peak places on reference point of mean velocity profile.

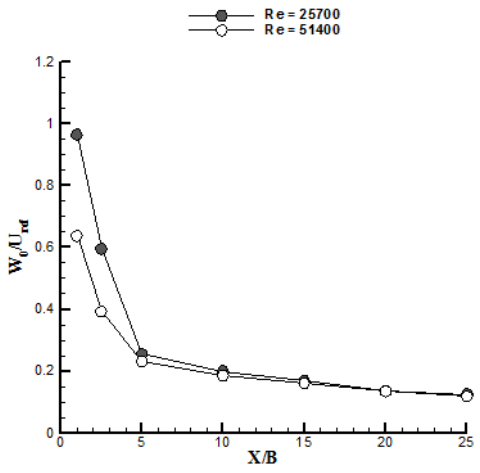

Figure 9 Variations of the dimensionless velocity defect for smooth cylinder

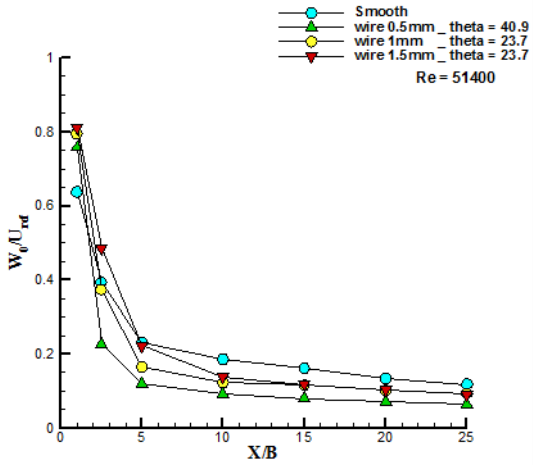

Figure 10 variations of the dimensionless velocity defect at different positions

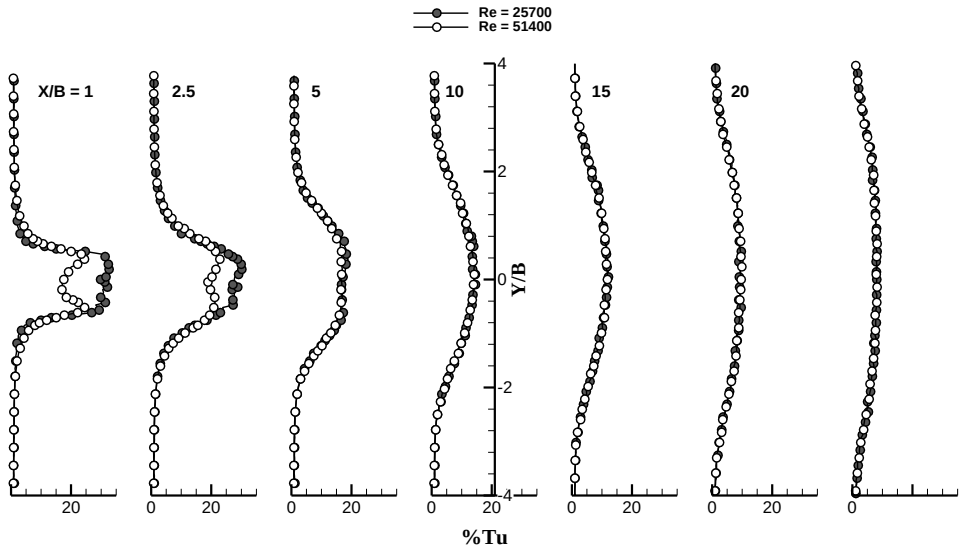

Figure 11 Distribution of the dimensionless turbulent intensity for smooth cylinder

The dotted line in Figure (12) is the half width line that passes the reference point of mean velocity profile. The line is determined for greater accuracy in recognizing how to adapt the profiles of mean velocity and turbulences flow in reference point of mean velocity profile. As it is determined, the peak of flow turbulences profile passes the reference point of mean velocity profile. In Figure (13) clear that the width of turbulences profile for smooth cylinder is more than the other profiles. This is because the separation point on a smooth elliptical cylinder occurs at the point higher than upstream, so the larger vortexes are created.

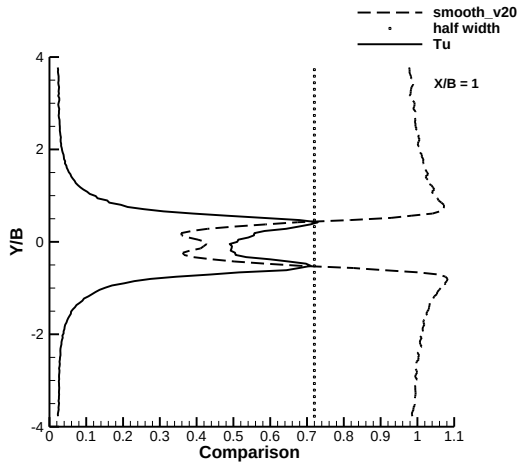

Figure 12 incidence of the peak of flow turbulences with reference point of mean velocity profile

As Figure (13) shows, turbulence profile for the situation $\theta = 40.9^{\circ}$ is smaller than the other turbulence profiles and the wake related to the cylinder in the presence of wire in this situation, is disappeared earlier than other states. Therefore, the turbulence peaks disappear earlier. In fact, in this case the wake has less width that it's eddies are weaker than others and therefore are destroyed earlier than other states. While for shrinking the width of the wake in the presence of trip wire a reattachment point for the formation of boundary layer farther from the downstream should happen that according to the Figure (13) this issue for position$\theta = 40.9^{\circ}$, better happened compared to the other positions. Because it's speed difference or the velocity defect on the wake is less than the other cases.

4.4 Strouhal number

Intensity of the vortex shedding frequency behind the model is determined by a dimensionless number called Strouhal number. As previously mentioned in relation 3, this number is stated as $St = {fd}/{U_{ref}}$ that f is vortex shedding frequency, d is large diameter of elliptic and finally U_{ref} is the free flow speed.

In fluid dynamics the vortex shedding is a fluctuation flow occurring when a fluid such as air or water passes on a bluff body at a specific speed that this shedding is dependent on the size and shape of the object. Pressure and lateral forces acting on the back of the cylinder in the frequency equal to the vibration frequency of eddy shedding in the back of model.[16]

Vortexes growth as well as the continuity and survival of their rotation, continue from the shear layer of wake and entering the flow lines into the wake causing their formation until the vortexes are enough powerful. By entering the flow lines into the wake, they fall in a low pressure area that is followed by low pressure vortexes. Because of energy dissipation, these vortices are broke down to smaller vortices along the wake and finally, Kolmogorov vortexes are created that are converted into heat energy directly as a result of depreciation.

On the other hand, if the object is not well installed and vortex shedding frequency get close to the oscillation frequency object and they be the same, the resonance will occur and therefore it can has destructive effects. As Figure (14) shows, the vortex shedding frequency for smooth cylinder in Reynolds number 51400 is a little more than the other. This difference is so small that it can be argued that changing the Reynolds number of flow has not a significant effect on Strouhal number in smooth cylinder.

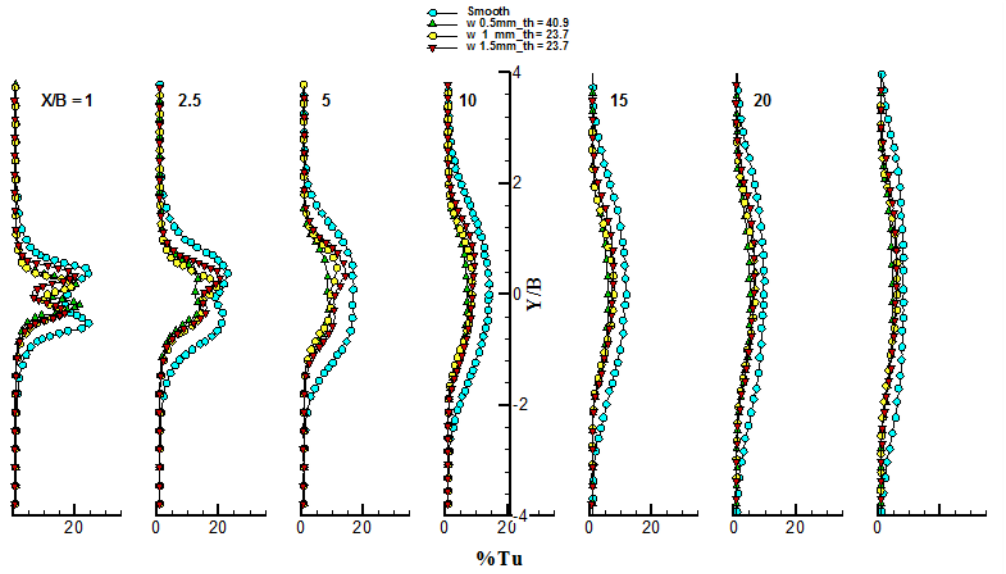

Figure 13 Distribution of the dimensionless turbulent intensity at different positions

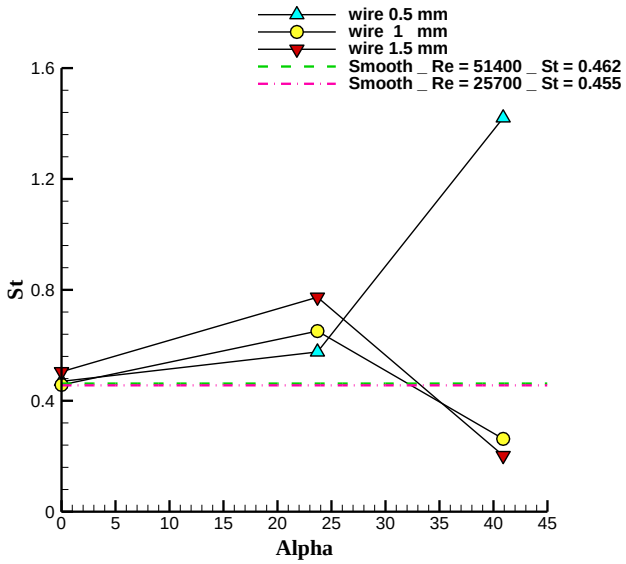

Figure 14 variations of the strouhal number at different positions

As is known, for 0.5 mm wire installation angle in situation $\theta = 40.9^{\circ}$ strouhal number compared to other diameters, has the largest values. The mean velocity on the wake in this position for wire 0.5 mm has the highest amount of speed implicating the most optimal conditions. It can be argued that the greater the amount of Strouhal number, the more favorable the situation of flow characteristics. It is clear that the impact of wire with a diameter of 1.5 mm in angle $\theta = 23.7^{\circ}$ from installing wire, is more than the other items.

4.5 Modifying the Schlichting's velocity defect profile

Herman Schlichting [17] around 1960 expressed a relationship for the wake of two-dimensional objects to far away stations where static pressure of wake is equal with their value outside the wake that based on it some equivalents for speed profile can be obtained in terms of velocity defect respect to the half width.

The main problem of this equation is its disability for stations close to the model that in this case is unusable. At this point, by adding two coefficients into the equation, it can be so optimized that mentioned equation will achieved with a very good approximation for each station that is expressed as follows:

$$\frac{U_{ref} - u}{U_{ref}} = \frac{S_1}{18 b_{1/2}} (10 C_D d)(1 - (\frac{S_2 y}{b_{1/2}})^{3/2})^2 \qquad (5)$$

Where d is the large diameter of the elliptic cylinder. In above equation, the S_1 correction coefficient changes the speed profile in direction of Y and S_2 correction coefficient changes the speed profiles in direction of X. Meantime, the S_{n} factor is defined as follows:

$$S_n = \frac{a C_D d}{X} \qquad n = 1,2 \qquad (6)$$

Where a coefficient can be changed based on the type of wire, its condition and current situations.

In Figure (15) a comparison between experimental results of speed profile of circular cylinder with a diameter of 2 cm with Angrili et al[18] at the station X/D = 2.5 and Reynolds number 24200 is implemented that an optimized equation for it is presented below.

$$\frac{U_{ref} - u}{U_{ref}} = 0.365 \left(1 - \left(0.692 \frac{y}{b_{1/2}}\right)^{3/2}\right)^2 \qquad (7)$$

In above relation, the a values obtained for S_1 is 750 and for S_2 is 37, respectively.

4.6 Survey of the drag coefficient

The drag force is consisted of two different types. The first type is pressure drag force. The pressure drag includes a large part of the total drag force in two-dimensional objects. In fact, using the trip wire, the flow is improved in order to reduce the pressure difference between the front and rear stagnation point of the model. Therefore, using trip wire followed by creating a

reattachment point, the wake width is decreased that cause increasing the pressure at back of the model. This increased pressure reduces the pressure difference on the model that consequently, the force exerted on the model is reduced through the pressure on it. However, Khan et al[19] indicated in an article about a smooth elliptical cylinder that Pressure drag coefficient is expressed by the following equation:

$$C_{D_p} = \int_0^{\pi} C_p \cos\theta \sqrt{1 - e^2 \cos^2\theta} d\theta \tag{8}$$

Where $e = \sqrt{1 - AR^2}$ is the centrifugal of elliptic and $AR = {}^{b}/_{a}$ is the axis ratio in which b is half diameter of the small elliptic and a is half diameter of large elliptic.

Another type of this force is called friction drag. The frictional drag due to viscous shear forces produced in the cylinder, resulting in the formation of the boundary layer on the surface of the cylinder. Drag coefficient of friction is expressed as follows:

$$C_{D_f} = \int_0^{\pi} C_f \sin\theta d\theta \tag{9}$$

Lu and Bragg[20] have a lot of research about the factors affecting the calculation of drag coefficient. They also examined the effects of turbulence and fluctuations of the flow and gained important results.

Van Dam[21] achieved an equation to calculate the drag coefficient in which were the Reynolds tension terms and the turbulence intensity of flow, but the changes in flow density and viscosity terms $\mu {}^{\partial u}/_{\partial x}$ were ignored. The components of equation are expressed as follows:

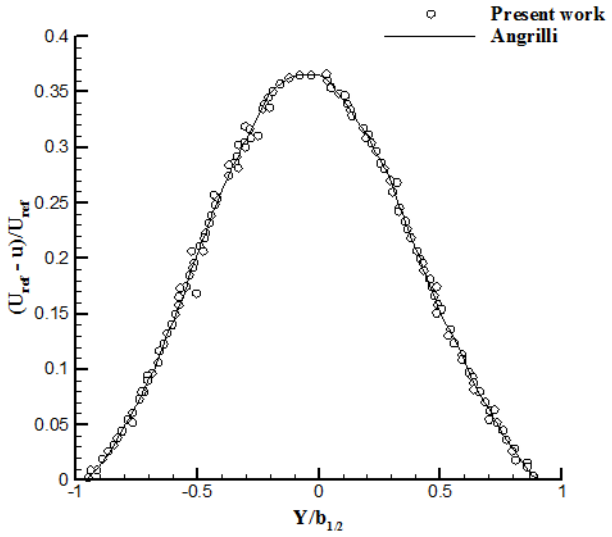

Figure 15 Angrilli et al at the station $X/D = 2.5$ and Reynolds number 24200

First component is related to pressure term:

$$\int_w \left(\frac{p_{s,e} - p_{s,w}}{q_{ref}}\right) d(\frac{z}{L}) \quad (10\text{-a})$$

Second component is related to momentum term:

$$2\int_w \frac{\bar{u}}{U_{ref}}(1 - \frac{\bar{u}}{U_{ref}}) d(\frac{z}{L}) \quad (10\text{-b})$$

Third component is related to Reynolds tension:

$$-2\int_w \frac{\overline{\acute{u}^2}}{U_{ref}{}^2} d(\frac{z}{L}) \quad (10\text{-c})$$

On the other hand, because the exact calculation of static pressure within the wake is a difficult task, therefore, based on several assumptions, the most important is that the average speed $\bar{v}$ and $\bar{w}$ are very small and ignorable and that the total pressure is constant along the streamline, the equation is simple. As a result the original Van Dam equation is as the ultimate form below:

$$C_d = 2\int_w \sqrt{\frac{\bar{q}}{q_{ref}}}\left(1 - \sqrt{\frac{\bar{q}}{q_{\mathrm{ref}}}}\right) d\left(\frac{z}{L}\right) + \frac{1}{3}\int_w \frac{\bar{\acute{q}}}{q_{ref}} d(\frac{z}{L}) \quad (11)$$

Where $\bar{\acute{q}} = \rho(\overline{\acute{u}^2} + \overline{\acute{v}^2} + \overline{\acute{w}^2})/2$ and it is assumed that far away from the downstream, the flow is homogenized and therefore $\acute{u} = \acute{v} = \acute{w}$. In the other hand, $\bar{q} = \frac{1}{2}\rho\bar{V}^2$ is the average time dynamic pressure and $q_{ref} = \frac{1}{2}\rho V^2$ is the dynamic pressure.

The method presented by Van Dam, based on its assumptions, is useful for steady flow and is restricted and contains errors for unsteady flow.

On the other hand, the drag coefficient of friction for the ratio of different axes $AR = a/b$ is presented as follows: [19]

$$C_{D_f} = \frac{1.353 + 4.43AR^{1.35}}{\sqrt{\mathrm{Re}_{\mathcal{L}}}} \quad (12\text{-a})$$

Where $\mathrm{Re}_{\mathcal{L}} = {}^{\mathcal{L}U_{ref}}/_{\nu}$ is the Reynolds number in which $\mathcal{L}$ is equal to large diameter of elliptic, $2a$. The pressure drag coefficient also is presented as follows:

$$C_{D_p} = (1.1526 + 1.26/\mathrm{Re}_{\mathcal{L}})AR^{0.95} \quad (12\text{-b})$$

Which eventually the total drag coefficient is equal to sum of pressure drag coefficient and friction drag coefficient that will be presented as follows:

$$C_{D_p} = \frac{1.353 + 4.43AR^{1.35}}{\sqrt{\mathrm{Re}_{\mathcal{L}}}} + (1.1526 + 1.26/\mathrm{Re}_{\mathcal{L}})AR^{0.95} \quad (13)$$

Using the Eq. (13) in comparison state in relation with present work, there is 0.65 percent errors for Reynolds number 25700 and 5.2 percent errors for another Reynolds number.

In Figure (16), the drag coefficient for Reynolds number 25700 is a bit higher than for others. This is because if the flow separation occurs too late, the wake width is reduced and therefore due to reduction of wake space, the pressure behind the model is increased and consequently the pressure difference is reduced for the model.[22]

However, the amount of $C_p = \frac{p_1 - p_2}{\frac{1}{2}\rho U_{ref}^2}$ in Eq. (8) is reduced by reducing this pressure difference. Because according to research of Khan, the $P_1 - P_2$ measures are equal to pressure difference in upstream and downstream levels of the flow in elliptic cylinder. So, according to Eq. (8), reducing the pressure difference causes reducing the drag coefficient.

As it's clear in Figure (17), the drag coefficient for wire with diameter of 0.5 mm is less than all other cases. If look at mean velocity charts in Figure (8), it is clear that the speed in wake for wire with diameter of 0.5 mm is more than the others. On the other hand, in Figure (13) it is clear that turbulence for this wire is less than others. Thus reducing the drag coefficient has a direct relationship with increasing the amount of mean velocity and reducing the flow turbulences. As it is clear, according to the Figures (14) and (17), for the lowest amount of drag coefficient obtained for wire of 0.5 mm at$\theta = 40.9^{\circ}$, also the most Strouhal number has occurred in this situation. On the other hand, at $\theta = 23.7^{\circ}$ is clear that the drag coefficient for wire 1.5 mm is less than its amount for wire 1 mm. While in Figure (14), the Strouhal number for wire 1.5 mm is more than the amount of the wire 1 mm.

However, for changes in Reynolds number of the flow for smooth elliptic cylinder, the drag coefficient does not change. Also there is a little change in Strouhal number because of changing the Reynolds number of the flow. Thus, by changing the Reynolds number of the flow, the drag coefficient and Strouhal number changes little in smooth cylinder. Ultimately, reducing the drag coefficient is proportional to increasing the Strouhal number.

Lindsey[23] has done a set of comprehensive research on drag coefficient of various objects in NASA experimentally. Meantime, the obtained results for smooth elliptic cylinder with an axis ratio of 1 to 2 with zero attack angle for different Reynolds numbers is as follows.

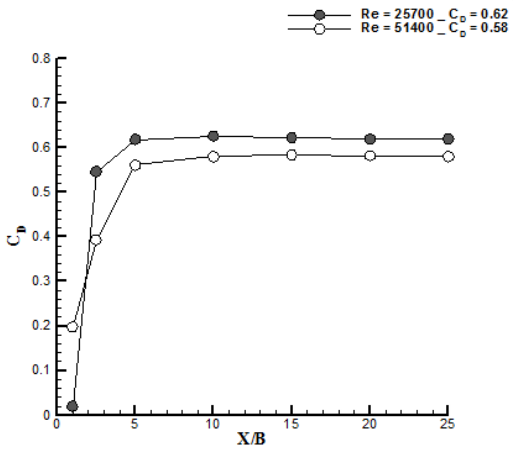

Figure 16 Variations of the drag coefficient for smooth cylinder at X/B

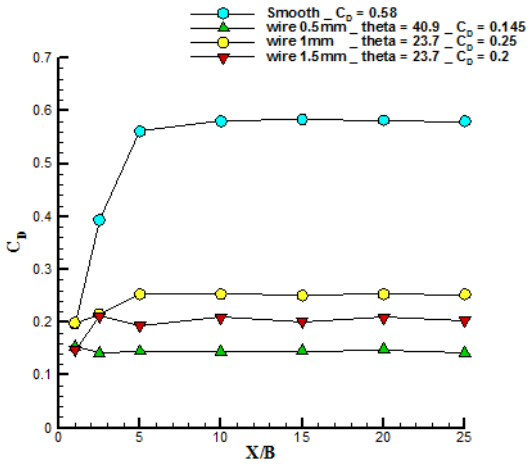

Figure 17 Variations of the drag coefficient at different positions at X/B

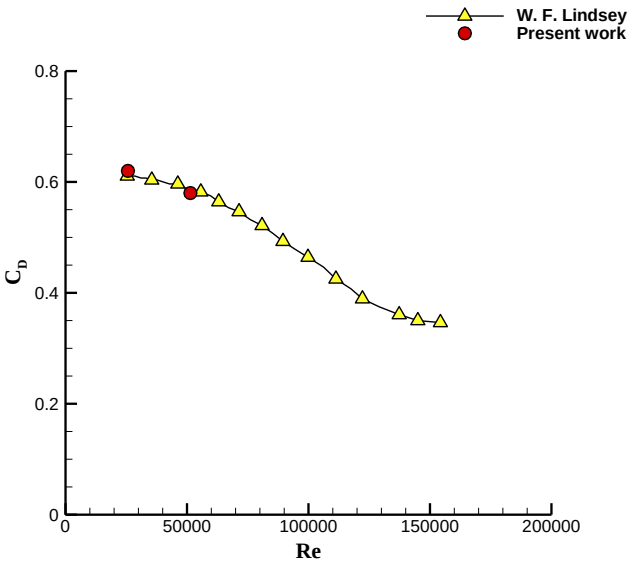

Figure 18 Variations drag coefficient at Reynolds number for elliptic cylinder

Considering that, so far, there is no research on the impact of trip wire on the wake of an elliptic cylinder. Therefore, as shown in Figure (18) only validating for data of smooth elliptic cylinder was possible.

5 Conclusion

This research is about study the direct effect of trip wire on the wake of a smooth elliptic cylinder with zero angle of attack that characteristics of flow wake are affected due to its presence.

In this study, an open-circuit wind tunnel and blower are used in order to make air flow and data capture stations have been selected in seven different places.

The results show that the trip wire has a significant effect on flow characteristics and reduction in current force and it strongly depends on the installation location of the wire on the model.

The results show that by increasing the Reynolds number of flow in a smooth cylinder, the drag coefficient is reduced. The result for the cylinder in the presence of wire depends on wire diameter and its position.
There was a sharp slope in dimensionless mean velocity profiles as well as in dimensionless turbulence intensity profiles for Reynolds number 25700 compared to Reynolds number 51400 in the smooth cylinder, suggests the fact that the rate of dissipation is higher in Reynolds number 25700. This causes an increase in the dissipation process of created vortexes behind the model in the flow.
Existence of sharp slope in profile of mean velocity is directly related to empowering the created vortexes behind the model. Another point is that reduction of drag coefficient is followed by increasing the mean velocity on the wake and also decreasing the amount of flow turbulences. On the other hand, it is clear that increasing the Strouhal number is directly related to reducing the drag coefficient. Therefore, reducing the flow turbulences in proportion to increasing the mean velocity in the wake causes the increasing of Strouhal number.
The structure of turbulence profile is so that turbulence peaks at stations close to the model pass from the reference point of mean velocity profile.
Another point is that reducing the drag coefficient is directly related to increasing the nusselt number of the flow. The results of this test may be useful to optimize a heat exchanger that its tubes are designed in elliptic cylinder shape to optimize it.

6 Error analysis

The effect errors of each parameter on speed can be calculated by the following equation, which is expressed as relative standard uncertainty (Jogensen 2002)

$$\text{Error}(\%) = \frac{1}{k} * \frac{1}{u} * \Delta y_i \tag{14}$$

K: Convergence coefficient

$$\frac{1}{u} * \Delta y_i : \text{Standard deviation}$$

Eventually, accumulation of errors stemming from different parameters affecting instantaneous speed can be calculated through the flowing equation:

$$\text{Error}(\%) = 2\sqrt{\sum(\frac{1}{k} * \frac{1}{u} * \Delta y_i)^2} \tag{15}$$

Errors occurring in the experiments include**:**

Maximum 1% error of manometer and Pitot tube calibration, up 1 percent error due to voltage curve fitting in terms of speed **,**maximum 0.12% error due to the uncertainty related to the conversion of analogue signals to digital, the error due to the position of the probe is negligible**.** Errors due to temperature changes, which consist of two parts: a _ a maximum of one degree of temperature change during calibration, the error volume is 0.003 percent. b _ changes in temperature during the test: a maximum of two degrees of temperature change during the test, which the error is 0.04%, the error caused by changes in humidity and atmospheric pressure that is negligible (Jogensen 2002). Considering all these factors, total measured error at the time of the test is 4.03 percent.

References

[1] Igarashi, T., "Effect of Vortex Generators on the Flow around a Circular Cylinder Normal to an Airstream", Bulletin of JSME, Vol. 28, pp. 274-282, (1985).

[2] Igarashi, T., "Effect of Tripping Wires on the Flow around a Circular Cylinder Normal to an Airstream", Bulletin of JSME, Vol. 29, pp. 2917-2924, (1986).

[3] Aiba, S., Ota, T., and Tsuchida, H., "Heat Transfer and Flow around a Circular Cylinder with Tripping-wires",Wärme - und Stoffübertragung, Vol. 12, Issue. 3-4, pp. 221-231, (1979).

[4] Zhou, C. Y., Wang, L., and Huang, W., "Numerical Study of Fluid Force Reduction on a Circular Cylinder using Tripping Rods", Journal of Mechanical Science and Technology, Vol. 21, pp. 1425-1434, (2007).

[5] Missirlis, D., Yakinthos, K., Palikaras, A., Katheder, K., and Goulas, A., "Experimental and Numerical Investigation of the Flow Field through a Heat Exchanger for Aero-engine Applications", International Journal of Heat and Fluid Flow, Vol. 26, Issue. 3, pp. 440-458, (2005).

[6] Hover, F. S., Tvedt, H., and Triantafyllou, M. S., "Vortex-induced Vibrations of a Cylinder with Tripping Wires", Journal of Fluid Mechanics, Vol. 448, pp. 175-195, (2001).

[7] Fukudome, K., Watanabe, M., Iida, A., and Mizuno, A., "Separation Control of High Angle of Attack Airfoil for Vertical Axis Wind Turbines", AIAA J., Vol. 50, pp. 3-5, (2005).

[8] Quadrante, L. A. R., and Nishi, Y., "Amplification/Suppression of Flow-induced Motions of an Elastically Mounted Circular Cylinder by Attaching Tripping Wires", Journal of Fluids and Structures, Vol. 48, pp. 93-102, (2014).

[9] Raman, S. K., Prakash, K. A., and Vengadesan, S., "Effect of Axis Ratio on Fluid Flow Around an Elliptic Cylinder—A Numerical Study", Journal of Fluids Engineering, Vol. 135, Issue. 11, pp. 111201-01 to 111201-10, (2013).

[10] Ota, T., Nishiyama, H., and Taoka, Y., " Flow around an Elliptic Cylinder in the Critical Reynolds Number Regime", Journal of Fluids Engineering, Vol. 109, Issue. 2, pp. 149-155, (1987).

[11] Paul, I., Prakash, K. A., and Vengadesan, S., "Numerical Analysis of Laminar Fluid Flow Characteristics Past an Elliptic Cylinder: A Parametric Study", International Journal of Numerical Methods for Heat & Fluid Flow, Vol. 24, Issue. 7, pp. 1570-1594, (2014).

[12] Perumal, D. A., Kumar, G. V. S., and Dass, A. K., "Lattice Boltzmann Simulation of Viscous Flow Past Elliptical Cylinder", CFD Letters, Vol. 4, No. 3, pp. 127-139, (2012).

[13] Alonso, G., Meseguer, J., Sanz-Andrés, A., and Valero, E., "On the Galloping Instability of Two-dimensional Bodies Having Elliptical Cross-sections", Journal of Wind Engineering and Industrial Aerodynamics, Vol. 98, Issue. 8-9, pp. 438-448, (2010).

[14] Flynn M. R., and Eisner, A. D., "Verification and Validation Studies of the Time-averaged Velocity Field in the Very Near-wake of a Finite Elliptical Cylinder", Fluid Dynamics Research, Vol. 34, Issue. 4, pp. 273-288, (2004).

[15] Alam, M. M., Sakamoto, H., and Moriya, M., "Reduction of Fluid Forces Acting on a Single Circular Cylinder and Two Circular Cylinders by using Tripping Rods", Journal of Fluids and Structures, Vol. 18, No. 3-4, pp. 347–366, (2003).

[16] Yaghin M. A. L., and Mojtahedi, A., "Hydrodynamic Parameter of Flow around a Cylindrical Pile and its Numerical and Experimental Modeling", Journal of Marine Engineering, Vol. 5, pp. 97-104, (2010).

[17] Schlichting, H., and Gersten, K., "*Boundary-Layer Theory*", 9th ed., Springer Press, Berlin, (2017).

[18] Angrilli, F., Bergamaschi, S., and Cossalter, V., "Investigation of Wall Induced Modifications to Vortex Shedding from a Circular Cylinder", Journal of Fluids Engineering, Vol. 104, Issue. 4, pp. 518-522, (1982).

[19] Khan, W. A., Culham, R. J., and Yovanovich, M. M., "Fluid Flow around and Heat Transfer from Elliptical Cylinders: Analytical Approach", Journal of Thermophysics and Heat Transfer, Vol. 19, No. 2, pp. 178-185, (2005).

[20] Lu, B., and Bragg, M. B., "Experimental Investigation of the Wake-survey Method for a Bluff Body with Highly Turbulent Wake", AIAA-3060, (2002).

[21] Dam, C. P. V., "Recent Experience with Different Methods of Drag Prediction", Progress in Aerospace Sciences, Vol. 35, Issue. 8, pp. 751-798, (1999).

[22] Behara, S., and Mittal, S., "Transition of the Boundary Layer on a Circular Cylinder in the Presence of a Trip", Journal of Fluids and Structures, Vol. 27, Issue. 5-6, pp. 702-715, (2011).

[23] Lindsey, W. F., "Drag of Cylinders of Simple Shapes", NACA Technical Report 619, pp. 169-176, (1938).

Nomenclature

AR =Axes ratio (proportion of small diameter to large diameter of elliptic)

B =Small diameter elliptic (m)

$b_{1/2}$=Half width (m)

C_{D_f}=Friction Drag coefficient

C_{D_p}=Pressure drag coefficient

C_{D}=Drag coefficient

C_f=Friction coefficient

C_p=Pressure coefficient

e =Eccentric elliptic

f =Vortex shedding frequency (s^{-1})

P_1=Front stagnation point pressure ($kgm^{-1}s^{-2}$)

P_2=Rear stagnation point pressure ($kgm^{-1}s^{-2}$)

Re =Reynolds number

St =Strouhal number

$\%Tu$ =The percentage of turbulence intensity

U_{ref}=Free-flow speed (ms^{-1})

u =wake flow speed (ms^{-1})

u_i=Horizontal component of free-flow speed (ms^{-1})

$\bar{u}$=Mean velocity (ms^{-1})

$\acute{u}$=Turbulent velocity fluctuation component (ms^{-1})

w_0=Velocity defect parameter (ms^{-1})

X =Distance from the rear stagnation point (m)

Greek symbols

β =Blockage ratio

μ =The dynamic viscosity ($kgm^{-1}s^{-1}$)

ρ =Density (kgm^{-3})

چکیده

در این تحقیق، رفتار و ویژگی های دنباله جریان در یک سیلندر بیضوی با زاویه ی حمله صفر درجه در حضور یک سیم اغتشاش ساز به صورت آزمایشگاهی مورد بررسی قرار گرفته است. برای این منظور، سیلندر آلومینیومی با مقطع بیضوی و محور اصلی و فرعی ۴۲,۴ و ۲۱,۲ میلیمتر و ارتفاع ۳۹۰ میلیمتر استفاده شده است. مدل سیلندر در بخش آزمون یک تونل باد دمنده مورد بررسی قرار گرفته است. عدد رینولدز نسبت به محور اصلی ۲۵۷۰۰ و ۵۱۴۰۰ برای سرعت ۱۰ متر بر ثانیه و سرعت ۲۰ متر بر ثانیه است.
سیمهای اغتشاش ساز با قطر ۰,۵ میلی متر، ۱ میلی متر و ۱,۵ میلی متر به صورت متقارن در هر دو طرف سیلندر قرار می گیرند، که در زاویه های صفر، ۲۳,۷ و ۴۰,۹ درجه نسبت به نقطه سکون بررسی شده اند. ضریب پسا برای سیلندر صاف برای اعداد رینولدز حدود ۰,۶ است. نتایج نشان می دهد که در بهترین حالت ممکن، ضریب پسا برای سیم ۰,۵ میلی متر، ۷۵٪ کاهش می یابد. در بهترین حالت، ضریب پسا به ترتیب برای سیم های ۱ میلی متر و ۱,۵ میلی متر نیز ۵۶,۹٪ و ۶۵,۵٪ کاهش می یابد.